



Research on the Test Section of High Fill Embankment in Swamp Soil of the Phase I Project of the Solo Kertosono Toll Road in Indonesia

Ganmeng Zhang*

CCCC FIRST Harbor Consultants Co., Ltd., Tianjin, China

*E-mail: 2879629717@qq.com

Abstract. This research project is based on the first phase of the toll road project from Solo to Kertosono in Indonesia, combined with a series of problems encountered during the construction process of the high-fill roadbed engineering in swampy soil. In response to key technologies during the construction process, a special study on the characteristics, bearing mechanism, and deformation law of swampy soil is carried out by using experimental sections. This article sorted out the engineering characteristics of the boundary moisture content, organic matter content, particle size, compression characteristics, and mechanical properties of the foundation soil at the project site, and analyzed the settlement law of the high-fill roadbed test section.

Keywords: Roadbed; Soft soil; Settlement

1 Introduction

1.1 Project location

The Phase I project of the Solo Kertosono Toll Road in Indonesia is located in East Java Province. It is part of the 178 km Solo Kertosono Toll Road and also part of the Jakarta Surabaya Expressway. The project connects Solo in Central Java to Kertosono in East Java, with a total length of approximately 37.39 km. The starting pile number is K139+610, and the ending pile number is K178+340. The K139+610-141+000 section is a hilly area and an excavation section. The K141+000-K178+340 (where K175+670-177+010 is a locally funded project and not within the scope of this construction) section is mainly filled with embankments, with mostly paddy fields along the way, densely populated villages, and flat terrain, forming a plain area^[1].

1.2 Engineering climate conditions

The project is located in a tropical rainforest climate with characteristics of high temperature, rainy weather, low wind, and humidity, with an average annual precipitation of over 1800 millimeters. Java Island has the most thunderstorms in the world, with an

© The Author(s) 2023

D. Li et al. (eds.), *Proceedings of the 2023 9th International Conference on Architectural, Civil and Hydraulic Engineering (ICACHE 2023)*, Advances in Engineering Research 228,

https://doi.org/10.2991/978-94-6463-336-8_45

average of approximately 220 thunderstorm days per year. Affected by the monsoon, each year can be divided into two seasons: dry and rainy^[2]. The rainy season in Java is from November to March of the following year, and the dry season is from April to October. The temperature changes very little in each month, without any distinction between cold and hot seasons, with an annual average temperature of 25-27°C. Surabaya City is the closest city to the construction site.

2 Research content

Due to the lack of engineering experience in the construction of high-fill subgrade in swampy soil, and the relatively complex natural and social environment of construction in West Java, Indonesia, the construction difficulty is relatively high. A 500 m test section needs to be established to verify the key construction technologies and construction processes proposed by the project department^[3]. In the experimental section, monitoring instruments such as pore water pressure gauges, water level gauges, settlement plates, and inclinometers need to be buried, and soil samples should be taken from the experimental area for experiments to verify and modify the simulation analysis results. We simulate the entire construction process of the high-fill roadbed through finite element software, and determine the deformation law and stability of the roadbed based on the calculation results, predicting the final settlement of the high-fill roadbed^[4].

3 Research on the subgrade test section

3.1 Indoor boundary moisture content test

Due to the incomplete parameters of the original roadbed soil in the geological survey report, supplementary geological investigation is needed. We drill holes at the foot of each section to obtain soil, with at least one drilling position not on the same side as the other two at the foot of the slope. The drilling depth is 30 m. After on-site soil sampling, we conduct laboratory indoor tests.

The liquid plastic limit, also known as the Atterberg limit, is two important physical indicators of cohesive soil, reflecting the sensitivity between soil particles and liquid water in the soil. The liquid limit refers to the boundary water content at which a soil mass transitions from a flowing state to a plastic state; the plastic limit is the boundary moisture content at which a soil mass transitions from a plastic state to a brittle state; the plasticity index refers to the range of changes in water content when the soil is in a plastic state, and its value is equal to the difference between the liquid limit and the plastic limit. The size of the plasticity index reflects to some extent the strength of the particle's ability to adsorb water^[5]. In cohesive soil, its plasticity mainly depends on the type and content of minerals that make up the clay particles (such as <0.005 mm). According to Skempton's research, activity indicators can be used to measure the ability of clay minerals in soil to adsorb water.

In general, the changes in dry shrinkage and wet expansion of cohesive soil are consistent with the changes in plasticity. The larger the liquid limit and plasticity index are, the worse the water stability is, and the greater the expansion and contraction performance of the soil is. The liquid plastic limit test of soil is to determine the two moisture contents or strengths of cohesive soil. When the moisture content increases, the strength of the soil decreases; when the water content decreases, the strength increases. When the water content of the soil is high, it will become soft and even flow like a fluid; on the contrary, the soil becomes harder and even exhibits brittle failure. Using a liquid plastic limit joint tester to measure the liquid plastic limit of the test section, it can be concluded that 1 and 2 Test sections are low liquid limit clay (with plasticity indices of 25 and 23), and Test 3 sections are high liquid limit clay (with plasticity indices of 9).

3.2 Compaction test

The quality of roadbed compaction is closely related to the quality of highway engineering, so the detection of roadbed compaction is an important part of highway quality inspection. The compaction degree of the roadbed is measured by the ratio of the actual dry density achieved on the construction site to the maximum dry density obtained from the indoor standard compaction test, which is the compaction degree or compaction coefficient. When determining the compaction standard, the maximum dry density and optimal water content are obtained by using indoor standard compaction tests^[6].

The compaction test provides two purposes for actual filling engineering: on the one hand, it is used to determine whether the soil's compaction performance is good under a certain compaction work, as well as the possible optimal compaction range, and corresponding optimal water content, providing a basis for the reasonable selection of filling water content and filling density for roadbed filling; on the other hand, it is to provide reasonable density and moisture content for preparing samples to study the mechanical properties of on-site fill. The most commonly used method to determine the maximum dry density is the compaction test method. The experimental principle is to prepare soil samples with different water contents, place them in a test cylinder, and compact them with a certain compaction function to obtain the relationship curve between water content and dry density. The optimal water content and corresponding maximum dry density are read out on the curve. According to the different compaction functions, compaction tests are divided into two types: light and heavy. In the early stages, due to poor compaction machinery and small driving loads, the compaction requirements for the roadbed were relatively low. The commonly used method was the light compaction method. With the development of rolling machinery and the increase in vehicle tonnage, the light compaction method has gradually been phased out, and the vast majority of current applications are heavy compaction methods. The compaction test is suitable for soil with particle sizes not greater than 38 mm. The maximum dry density of the sampled samples from the experimental section is shown in Test 1: 16.3 (kN/m³), Test 2: 16.1 (kN/m³), Test 3: 17.8 (kN/m³).

The moisture content in soil has a significant impact on the compaction effect. When the water content is low, due to the attraction between soil particles, which may also

include capillary pressure, the soil maintains a relatively loose state or cohesive structure. The pores in the soil are mostly interconnected, with less water and more gas. Under a certain external compaction function, although the gas in the soil pores is easily expelled and the density may increase, the lubrication effect of the water film is not obvious, the external work is not enough to overcome the attraction between particles, and the soil particles are not prone to relative movement, so the compaction effect is relatively poor. When the water content increases, the water film thickens, the gravity decreases, and the water film plays a lubricating role. The external compaction function makes it easier to cause the soil particles to move, resulting in the best compaction effect; when the water content is too high, free water appears in the pores, and the compaction function cannot discharge the gas. A part of the compaction function is offset by free water, reducing the effective pressure and the compaction effect. Whether the moisture content is too high or too low will affect the compaction effect, and the compaction effect is best only when the moisture content is the most suitable, that is when the soil moisture content is optimal. The optimal moisture content of the soil samples from the experimental section is shown as Test 1: 19%, Test 2: 20%, and Test 3: 17%.

3.3 Analysis of monitoring results in the experimental section

The monitoring instrument for the experimental section is an inductive single-point settlement meter, which is installed by using a drilling method. The settlement meter model used in this project is JMDL4740, with a range of 400 mm and a sensitivity of 0.1 mm. It has functions such as intelligent memory and automatic storage. That is, the displacement value can be intelligently displayed through the reading instrument, which can be used to study the on-site testing of the roadbed (Fig.1).

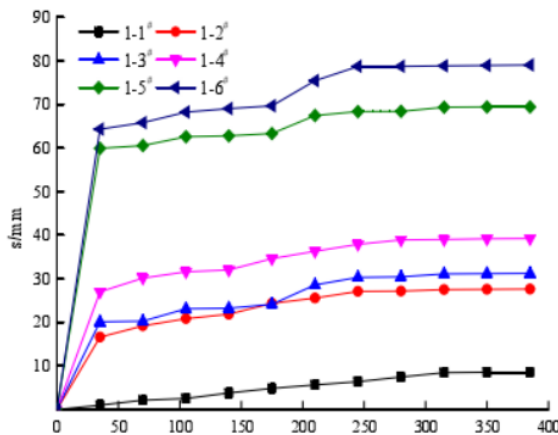


Fig. 1. Curve of shoulder settlement versus time

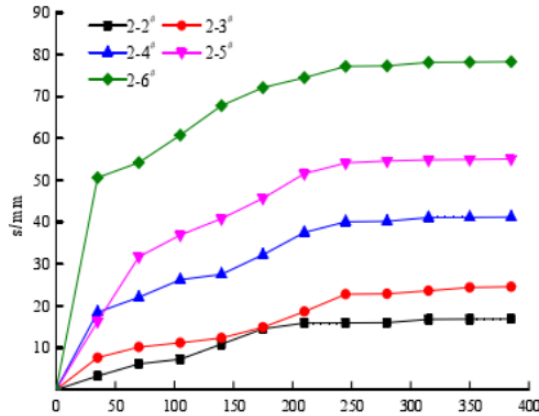


Fig. 2. Curve of settlement and time of overtaking lane

According to the shoulder settlement curve in Figure 2, it can be seen that the overall settlement value of monitoring points 1 to 1 # is the smallest, followed by the settlement value of 1 to 2 #, and the overall settlement value of 1 to 6 # is the largest. The overall analysis of its settlement trend shows that the curve shape is similar, and the settlement amount increases with time. The settlement amount increases linearly from 0 to 40 days, and then the settlement curve increases slowly until around 250 days and tends to stabilize; because the monitoring started in autumn and entered winter three months later, climate change may lead to freeze-thaw phenomena, resulting in fluctuations in settlement; the maximum settlement corresponding to the shoulder position is 79.03 mm, the minimum is 8.60 mm, and the average settlement value is 43.82 mm. Therefore, for predicting the post-construction settlement of the road shoulder in actual engineering, the average settlement of its monitoring points can be referred to.

From the settlement curve of the overtaking lane in Figure 3, it can be seen that the settlement of monitoring points 2-2 # is the smallest, followed by 2-3 #, and 2-6 # has the largest settlement. That is to say, the minimum filling depth is 6 m, followed by 9 m, and the maximum filling depth is 18 m. The overall analysis of its settlement trend shows that the curve shape is basically similar, and the settlement amount increases with time. The settlement amount increases linearly from 0 to 40 days and then increases slowly, and the settlement tends to be flat after about 250 days. Due to significant seasonal differences between the start of monitoring and the last monitoring, climate change may lead to changes in road settlement values; the maximum settlement corresponding to the overtaking lane position is 78.28 mm, and the minimum is 16.88 mm, resulting in an average settlement value of 47.58 mm. Therefore, for predicting the road settlement at the overtaking lane position in practical engineering, the average settlement at its monitoring points can be referred to.

In summary, by comparing Figures 2 and 3, it can be seen that the overall settlement of the shoulder position is greater than the settlement of the passing lane, which is related to the lack of lateral constraints on one side of the shoulder and constraints on both sides of the passing lane. Comparing the settlement of the shoulder and overtaking

lane, the settlement at the shoulder is the smallest at a depth of 3 m for the filling body and the largest at a depth of 18 m. The settlement of the filling body first increases, then decreases, and finally tends to be gentle. The slope of the settlement curve at 0-40 d is relatively large, indicating that the settlement rate has been increasing, accounting for 80% of the total settlement. The settlement value between 40 d and 160 d continues to increase, while the change in settlement rate gradually decreases and reaches its peak at 160 d; the settlement rate changes gradually from 160 d to 250 d, and tends to stabilize gradually around 250 d.

4 Simulation analysis

We select drilling holes 177+750 for calculation. The depth of the foundation soil in this section is 60 m, and according to the data, the road foundation is 7 m. The consolidation coefficient of this borehole under load is $9.13 \times 10^{-3} \text{ cm}^2/\text{s}$. The soil weight within the depth range of 0-5 m is 1.81 t/m^3 , and the soil weight within the depth range of 6-10 m is 1.63 t/m^3 . This calculation uses PLAXIS 3D for simulation analysis, which can fully simulate the three-dimensional effect of the roadbed and analyze the anti-slip and reinforcement effects of geotextile in the roadbed^[7]. The calculation model is shown in Figure 3.

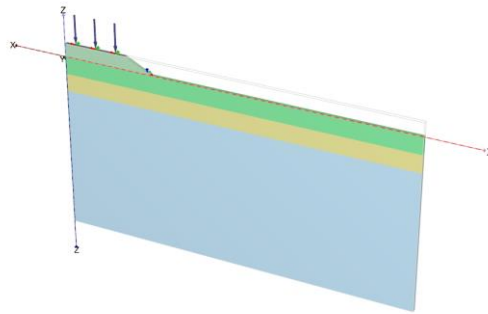


Fig. 3. PLAXIS 3D computing model

4.1 Actual engineering situation of geotextile

This simulation simulated the construction project of filling and rolling the roadbed seal layer, taking into account the influence of the consolidation time of the roadbed soil during the construction process, and analyzed the impact of the negative load on the roadbed settlement after the trial operation of the highway. According to calculations, after the completion of the first layer of roadbed filling construction, the roadbed settlement is 5 cm, and after the completion of roadbed and pavement construction, the total settlement is 19.6 cm. When the highway operates normally, the total settlement of the roadbed is about 26 cm.

In addition, to analyze the impact of geotextiles on roadbed settlement and roadbed slope stability, the safety coefficient of the roadbed was calculated. The calculation

results of the stress concentration point of the roadbed are shown in Figure 4, and the shape of the roadbed slip arc in the presence of geotextiles is shown in Figure 5. According to calculations, it can be found that the stress concentration points of high-fill roadbeds are divided into two parts. One part is within 5-10 m below the road surface, and the other part occurs at the junction of the roadbed slope foot and the original road surface. If the roadbed is too high or the road load is too large, shear damage will occur at the roadbed slope foot. Drainage and filtration measures should be taken, and for soft soil roadbed, back pressure should also be taken at the slope foot.

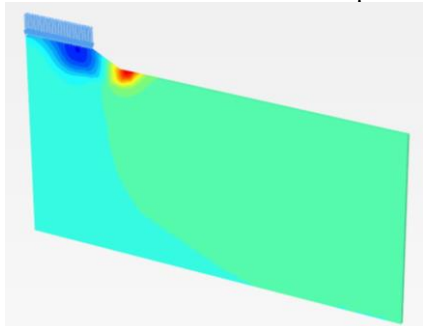


Fig. 4. Calculation results of stress concentration points in the roadbed

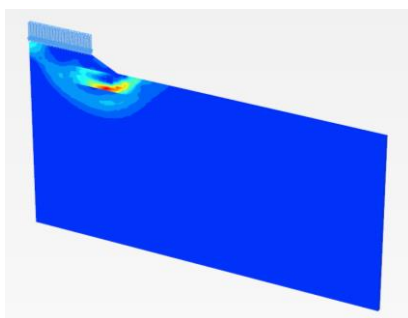


Fig. 5. Shape of roadbed sliding arc with geotextiles

4.2 No geotextile engineering situation

To compare the impact of the presence or absence of geotextile on shoulder stability, this calculation only calculates the safety factor of shoulder anti-slip stability. The strain cloud diagram of shoulder anti-slip stability in the absence of geotextile is shown in Figure 6. According to the calculation, in the absence of geotextile, the roadbed is prone to generating circular arcs that penetrate the sliding surface, leading to instability of the roadbed under excessive load. Through calculation and comparison, it is found that the presence or absence of geotextile has little impact on the total settlement of the roadbed. However, for settlement during construction, geotextile can better ensure the integrity of the roadbed, increase the settlement of the original roadbed soil during the

construction process, and have a strong effect on improving the stability of the roadbed slope.

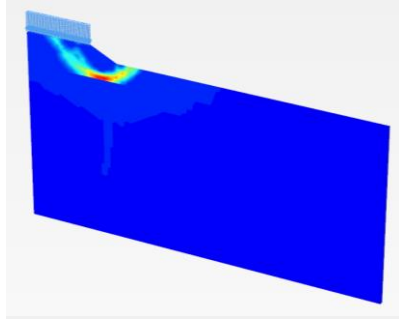


Fig. 6. Strain for shoulder sliding stability without geotextiles

5 Conclusion

This article introduces the engineering characteristics of the boundary moisture content, organic matter content, particle size, compression characteristics, and mechanical properties of the foundation soil where this project is located. We embed detection instruments such as pore water pressure gauges, settlement plates, water level gauges, and inclinometers in the experimental section of roadbed filling to ensure the safety of the filling process and select appropriate data collection frequencies to monitor the construction process. We obtain physical and mechanical indicators, as well as consolidation and permeability performance indicators of swamp soil.

The settlement monitoring instruments used in the experimental section were described in detail, including the layout of monitoring points, the burial and installation of settlement meters, testing methods, and the collection method of test data. Based on the on-site measurement of the high-fill roadbed using a single-point settlement meter, the settlement law is analyzed and obtained.

This article also uses finite element software to simulate the entire construction process of the high-fill roadbed, and determines the deformation law and stability of the roadbed based on the calculation results, predicting the final settlement of the high-fill roadbed.

References

1. MESRI G, AJLOUNI M A. Engineering properties of fibrous peats [J]. *Journal of Geotechnical and Geoenvironmental Engineering*, 2007, 133(07): 850–866.
2. Skempton A W, Petley D J. Ignition Loss and other properties of peats and clays from Avonmouth, King's Lynn and Cranberry Moss[J]. *Geotechnique*, 1970, 20(4): 343-356.
3. Meng Xianqin. Experimental Study on Settlement of High Fill Roadbed [J]. *Urban Roads and Bridges and Flood Control*, 2001, 20(1): 102-105

4. Jiang Zhongxin, Chen Guofang, Zhang Limin. Simulation Analysis of the Settlement of Qidian Peat Soil Roadbed on the Nankun Railway [J]. *Subgrade Engineering*, 1999, 87(6):24-28.
5. Bai Wulong, Lu Yongcheng. Analysis of the Mechanical Characteristics of the Pier Top Connection Section of Jakarta Elevated Simple Supported to Continuous Small Box Girders in Indonesia [J]. *Urban Roads Bridges and Flood Control*, 2019(2):6. DOI: 10.16799/j.cnki.csdqyfh.2019.02.018.
6. Su Guanghui. Causes and Comprehensive Prevention Measures for Cracks in Mud Concrete Pavement: Taking the CISUMDAWU Highway Project in Indonesia as an Example [J]. *Engineering and Technological Research*, 2021, 6(15):2.
7. Zhang Hailing. Research on Construction Treatment Technology of Roadbed in Settlement Section of Highway Bridges [J]. *Engineering Technology*, 2022(9):3.

Open Access This chapter is licensed under the terms of the Creative Commons Attribution-NonCommercial 4.0 International License (<http://creativecommons.org/licenses/by-nc/4.0/>), which permits any noncommercial use, sharing, adaptation, distribution and reproduction in any medium or format, as long as you give appropriate credit to the original author(s) and the source, provide a link to the Creative Commons license and indicate if changes were made.

The images or other third party material in this chapter are included in the chapter's Creative Commons license, unless indicated otherwise in a credit line to the material. If material is not included in the chapter's Creative Commons license and your intended use is not permitted by statutory regulation or exceeds the permitted use, you will need to obtain permission directly from the copyright holder.

